

Air Bumper: A Collision Detection and Reaction Framework for Autonomous MAV Navigation

Ruoyu Wang, Zixuan Guo, Yizhou Chen, Xinyi Wang, Ben M. Chen

Abstract—Autonomous navigation in unknown environments with obstacles remains challenging for micro aerial vehicles (MAVs) due to their limited onboard computing and sensing resources. Although various collision avoidance methods have been developed, it is still possible for drones to collide with unobserved obstacles due to unpredictable disturbances, sensor limitations, and control uncertainty. Instead of completely avoiding collisions, this article proposes Air Bumper, a collision detection and reaction framework, for fully autonomous flight in 3D environments to improve the safety of drones. Our framework only utilizes the onboard inertial measurement unit (IMU) to detect and estimate collisions. We further design a collision recovery control for rapid recovery and collision-aware mapping to integrate collision information into general LiDAR-based sensing and planning frameworks. Our simulation and experimental results show that the quadrotor can rapidly detect, estimate, and recover from collisions with obstacles in 3D space and continue the flight smoothly with the help of the collision-aware map.

I. INTRODUCTION

MAVs have gained increasing popularity for their ability to access and operate in environments that are difficult or impossible for humans to reach, making them valuable tools in various fields like infrastructure inspection [1]–[3], subterranean exploration [4]–[6], and search and rescue [7], [8], etc. However, safety becomes a critical concern for MAVs when operating in such complex and cluttered environments. These scenarios present a significant challenge for MAVs to conduct safe and collision-free flights. To address this challenge, much research has focused on utilizing onboard sensors such as LiDAR [9], stereo cameras, and RGB-D cameras [10] for Simultaneous Localization and Mapping (SLAM); motion planning algorithms [11], [12] have been developed to generate collision-free paths. Despite these efforts, MAVs are still susceptible to colliding with obstacles due to unpredictable disturbances, sensor limitations, and control uncertainty.

Instead of dealing with MAV collision by completely avoiding it, increasing attention has been shifted to collision detection and reaction. In this paper, we introduce a unified IMU-based collision detection and reaction framework (Air Bumper) that estimates collision points and feeds the collision information into collision-aware volumetric mapping and general motion planning algorithms so that robots can move to the original target rather than get stuck by obstacles.

The work was supported in part by the Research Grants Council of Hong Kong SAR under Grants 14209020 and 14206821, and in part by the Hong Kong Centre for Logistics Robotics. Authors are with the Chinese University of Hong Kong, Shatin, N.T., Hong Kong 999077. (Email: {rywang, zxguo, josephchen, xywangmae}@link.cuhk.edu.hk, bmchen@cuhk.edu.hk).

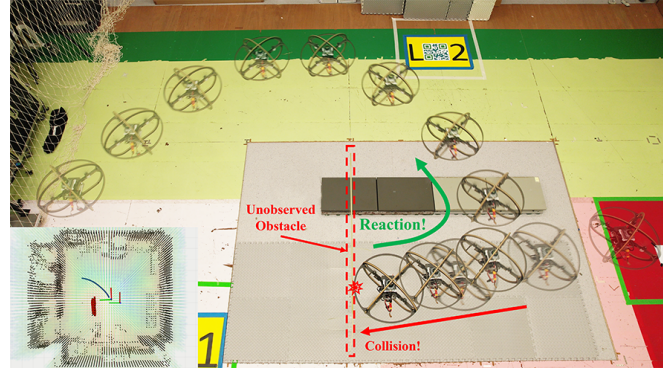


Fig. 1. Illustration of a collision detection and reaction experiment with Air Bumper.

The collision detection and estimation only rely on IMU data from the flight controller without requiring any external sensors. We also design and fabricate a fully-autonomous collision-resilient MAV with a 3D cage. The drone runs Air Bumper, the proposed IMU-based collision detection and reaction framework, in addition to general autopilot, SLAM, and motion planning algorithms. The proposed framework enables the drone to detect and react to unobserved collisions and update a collision-aware map for autonomous navigation after collisions (Fig. 1).

The main contributions of this work are:

- We propose Air Bumper, an IMU-based collision detection and reaction framework for autonomous MAV navigation in 3D environments.
- We propose a collision-aware mapping method to utilize collision estimation as sensor information in the general autonomous navigation framework.
- We design and fabricate a collision-resilient MAV that can autonomously navigate in unknown environments while sustaining collisions with obstacles.

The rest of this paper is organized as follows. In Section II, we review state of the art on MAV collision detection and reaction. In section III, we introduce our overall framework's structure and the design of a fully-autonomous collision-resilient MAV. The IMU-based 3D collision detection and reaction methods are detailed in Section IV and V, respectively. The simulation and experiment results that demonstrated the performance of Air Bumper are presented in Section VI. Finally, we draw some conclusions in Section VII.

II. RELATED WORKS

In the face of possible collisions in flight, many researchers choose not to generate a collision-free path to avoid the

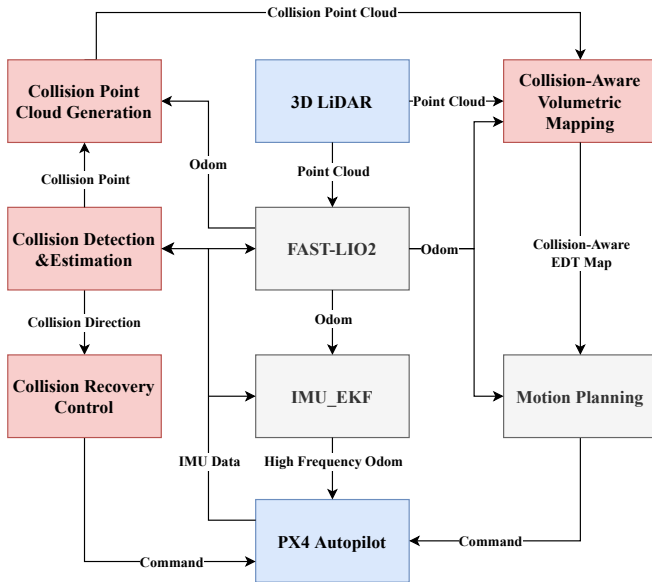


Fig. 2. Overview of the collision detection and reaction framework.

collision but to design collision-resilient MAVs to deal with it. At the hardware level, there are many kinds of designs and structures to enhance collision resilience. As a high-speed rotating part, the propeller is the most vulnerable to damage in a collision. Therefore, propeller guards [13]–[15] are commonly used to protect it. At the same time, many cage-like structures are designed to provide more protection for the whole drone. Rigid cage structure [16], [17] can use its strength to protect inside fragile parts, like sensors, flight controllers, and onboard computers.

In addition to minimizing the impact of collisions through the hardware design discussed above, some researchers are also extracting environmental information from collisions in order to integrate it into the MAV perception system. Lew et al. in [18] proposed a contact-based inertial odometry (CIO), which can provide a usable but inaccurate velocity estimation for a hybrid ground and aerial vehicle performing autonomous navigation. In the flight, several not destructive collisions happen, and the controller can get updated information from collisions. The work in [19] analyzes the impact of collisions on visual-inertial odometry (VIO) and uses collision information to build a map with a downward camera for localization. In their experiment, two glass walls are included to present that the transparent objects may cause LiDAR to get an inaccurate distance. Still, collision mapping can help MAVs detect these transparent walls. Authors in [14], [20] introduce hall sensors to detect collisions and estimate the intensity and location of the collision to realize reaction control. However, these works tend to navigate using only IMU or directly use collision data to perform reaction control, which makes the collision information hard to be recorded and reused. Although the method proposed in [15] successfully achieves collision recording for further flight in a laboratory environment using motion capture systems, the lack of integration with online sensing and planning modules

limits its applicability in real-world settings. Additionally, most of these works [21], [22] focus on collision detection and characterization in a 2D environment. However, the obstacles in cluttered environments are often not on the same level as MAVs, which means that collisions can occur from any direction. In this work, we combine the Air Bumper framework with LiDAR-based sensing on a caged, collision-resilient MAV. This allows for collision detection and estimation in 3D space and the generation of smooth reaction trajectories with the help of collision-aware mapping.

III. SYSTEM OVERVIEW

A. Overview of Air Bumper Framework

The structure of our proposed collision detection and reaction framework, Air Bumper, is shown in Fig. 2. When MAV is flying in unknown environments, it may collide with obstacles due to the onboard sensors' limitations. In this condition, the collision detection part of our framework will use inertial data from the flight controller to estimate the collision points and feed the collision information into collision reaction modules. In collision reaction parts, the collision recovery control algorithm will utilize the direction of the collision point to command the MAV away from obstacles. Meanwhile, it will also generate a collision point cloud to the collision-aware mapping module so that the position of unobserved obstacles can be stored for further navigation. Using the updated collision-aware map, a general motion planning system can easily get the ability to deal with unobserved obstacles in 3D environments.

B. Design of Collision-Resilient MAV



Fig. 3. Overview of the design of the caged collision-resilient MAV.

The collision resilient MAV, shown in Fig. 3, is designed and fabricated using a customized frame and cage made of carbon fiber composite material [16], [17], 3D printed parts, and commercial electrical components. The quadrotor weighs 1.45 kg with a battery and 3D LiDAR. The frame and cage of the MAV are made of a composite material consisting of carbon fiber and PVC foam, which provides full coverage for onboard components while keeping the entire MAV lightweight. The counter of the frame is designed as circular, which makes the collision estimation more efficient and accurate. An autopilot, Kakute H7, is utilized as the low-level controller. NVIDIA Xavier NX module with carrier board is chosen as the onboard computer for high-level

control, providing computing capabilities for Air Bumper, GPU-accelerated volumetric mapping, and motion planning algorithms. The whole MAV is powered by an ACE 4-cell 45C 5300 mAh LiPo battery. Livox Mid-360 LiDAR sensor has been selected to enable 360° of horizontal field of view (FOV) and 59° of vertical FOV. This allows for precise point cloud data collection and navigation in indoor environments.

The collision-resilient MAV integrates state-of-the-art flight control, localization, and mapping techniques to achieve fully autonomous and safe flight in unknown environments. The autopilot using PX4 firmware receives pose estimation and targets and runs a low-level controller to generate actuator commands. Robot Operating System (ROS) framework runs on the onboard computer for high-level algorithms. FAST-LIO2 [9] SLAM algorithm is chosen to provide odometry data. To meet the required frequency, the framework employs an Extended Kalman filter (EKF) to fuse the odometry data with the onboard IMU. The high-frequency odometry (200Hz) is then used by autopilot. A volumetric mapping module [23] provides GPU-accelerated incremental euclidean distance transform for corresponding online motion planning [12]. The volumetric mapping module is modified to work with collision-aware map in the Air Bumper framework.

IV. IMU-BASED COLLISION DETECTION AND ESTIMATION IN 3D SPACE

A. Collision Detection

To make Air Bumper easier to implement on any platform, IMU, the most common drone sensor, is used to collect linear acceleration data on x , y , and z axes to detect the collisions rapidly. When the collision happens, the contact force will cause an additional acceleration on the MAV, and the measured value on the corresponding axes will significantly differ from the normal state. Different from the previous work [14], [15], [19], they only consider detecting the collision on a horizontal plane or using acceleration data on the z -axis to assist the horizontal detection. Our method also takes into account collisions other than those from horizontal planes. This feature can assist popular caged MAVs in detecting collisions from any angle. Let ${}^b\mathbf{a}$ as the acceleration vector of the MAV.

Based on the analysis of acceleration data, we found that an acceleration sample can be identified as a potential collision signal if the magnitude of its component on either the x or y axis, represented as $|{}^b\mathbf{a}_x|$ or $|{}^b\mathbf{a}_y|$, exceeds a threshold of 20 m/s². The relative threshold for collision detection on the z -axis is also 20 m/s², but the gravitational acceleration must be added. Meanwhile, the impact of a collision on MAV may cause several related abnormal acceleration data samples. To realize robust collision detection and estimation, a sliding-window method is used to select the maximum value from ten samples following the first acceleration data that exceeds the threshold. After the selection, the represented data sample for one collision will be recorded. In the collision detection stage, we only set the threshold and the

size of the sliding window to filter the sensor noise and post-impact of collision, which can be easily adjusted according to specific hardware.

B. Collision Estimation

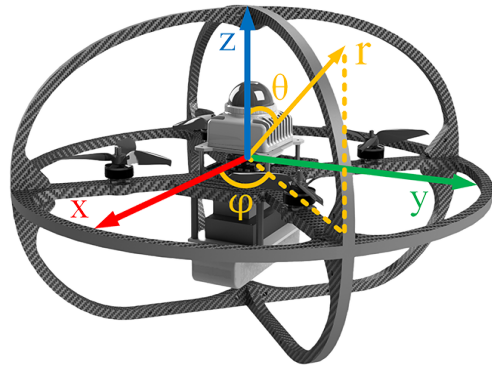


Fig. 4. Demonstration of the intensity and direction of a collision ${}^b\mathbf{C}$.

The collision estimation module estimates the intensity and direction of collision ${}^b\mathbf{C}$ in the body frame for collision recovery control. It also outputs a collision point ${}^b\mathbf{p}_c$ for generating a collision point cloud. We represent the intensity of collision ${}^b\mathbf{C}$ using r . And the collision direction is represented using azimuth angle $\phi \in (-\pi, \pi]$ and polar angle $\theta \in [0, \pi]$. The acceleration directions are the opposite of the directions of collision points in the body frame. Therefore, we can represent the acceleration value as a collision acceleration vector \mathbf{a}_c , where $a_{c,x} = -{}^b a_{c,x}$, $a_{c,y} = -{}^b a_{c,y}$, $a_{c,z} = -({}^b a_{c,z} - g)$. Then, we can estimate the collision via

$$r = \sqrt{{}^b a_{c,x}^2 + {}^b a_{c,y}^2 + {}^b a_{c,z}^2} \quad (1)$$

$$\phi = \text{atan2}({}^b a_{c,y}, {}^b a_{c,x}) \quad (2)$$

$$\theta = \arccos \frac{{}^b a_{c,z}}{r} \quad (3)$$

The collisions between the aircraft and the obstacle occur on the edge of the drone's cage. To update a collision-aware map for navigation, we need to estimate a collision point ${}^b\mathbf{p}_c$ on edge. For simplicity, we assume that the cage of our drone is a sphere with a radius l . Then the collision point can be estimated by:

$${}^b\mathbf{p}_c = \frac{{}^b\mathbf{C}}{\|{}^b\mathbf{C}\|} \cdot l \quad (4)$$

V. COLLISION REACTION IN 3D SPACE

Our collision reaction method aims first to utilize a simple but rapid recovery control strategy to quickly guide the MAV away from obstacles and restore its stability. Then, the collision mapping module transfers the collision point into a corresponding collision point cloud and integrates it with a volumetric mapping algorithm. This enables the robot to record the estimated positions of obstacles in the world frame and navigate to the pre-collision goal using general motion planning algorithms.

A. Collision Recovery Control Strategy

When the collision occurs, the MAV without our framework will maintain its target velocity but cannot achieve it. The motors will continue to accelerate and lead the robot to crash. The collision recovery control strategy generates a target position on the opposite side of the collision point to address this condition rapidly. Instead of relying on the motion planning module, which typically requires time to re-plan, the position command is sent directly to the low-level controller. Firstly, we need to get the collision recovery position ${}^b p_r$ in the body frame as follows:

$${}^b p_{r,x} = -d \sin \theta \cos \phi \quad (5)$$

$${}^b p_{r,y} = -d \sin \theta \sin \phi \quad (6)$$

$${}^b p_{r,z} = -d_z \cos \theta \quad (7)$$

where d is the reaction distance in the xy -plane, d_z is the reaction height on the z -axis. The collision recovery position in the world frame is denoted by ${}^w p_r = {}^w T_b \cdot {}^b p_r$, which utilizes a transform matrix, ${}^w T_b$, to achieve the transformation from the body frame to world frame. We limit the reaction distance or height to keep the MAV a safe distance away from the obstacles rather than directly use the collision intensity r , as the acceleration caused by collisions can often be very large. Then a standard cascaded proportional–integral–derivative (PID) controller is used to generate thrust force commands from the desired reaction positions.

B. Collision Point Cloud Generation

The collision point cloud generation module is designed to record the positions of unobserved obstacles and avoid a secondary collision. This module constructs a set of points to fit the collision plane where the drone detects the collision. The collision point cloud is then registered in the global volumetric map for the motion planning algorithm to avoid invisible obstacles when re-planning the feasible path autonomously.

Firstly, we assume the object that collides with the surface of the drone is a circular plane with radius r_c and center point p_0 . r_c is related to the geometric information of the MAV, while $p_0 = (x_0, y_0, z_0)$ is given by the collision point ${}^b p_c$ which is generated by the collision estimation module. The 3D collision circular plane can be constructed as an intersection of a sphere, and a plane follows the equation 8.

$$\begin{aligned} (x - x_0)^2 + (y - y_0)^2 + (z - z_0)^2 &= r_c^2 \\ x_0(x - x_0) + x_0(y - y_0) + x_0(z - z_0) &= 0 \end{aligned} \quad (8)$$

With the guidance of equation 8, a sphere point cloud ${}^b P_{sph}$ can be generated with the help of point cloud library (PCL), and then each point in ${}^b P_{sph}$ will check whether the plane fitting condition is satisfied. Finally, the selected points are used to construct the 3D collision circle plane point cloud ${}^b P_{cir}$. Then the point cloud is converted to the world frame using ${}^w P_{cir} = {}^w T_b \cdot {}^b P_{cir}$ for building a collision-aware map.

C. Collision-Aware Mapping

For autonomous navigation purposes, we represent the environment with the help of a volumetric mapper [23]. The mapping system constructs Occupancy Grid Maps (OGMs) and Euclidean Distance Transforms (EDTs) by parallel computing in GPU. An OGM contains the probability of a voxel (an element of the 3D grid) being occupied by obstacles, while an EDT consists of structural voxel grids where every voxel contains the distance information to its closest obstacle.

The mapper reads the input data of depth and poses from onboard sensors and constructs OGM incrementally. Within the local range, a parallel EDT algorithm converts a batch of OGM in the local volume to EDT. In detail, given a 3D voxel v , the distance value is computed in the way

$$f(v) = \min_{u \in O} \|u - v\| \quad (9)$$

where O denotes the set of voxels that are occupied. Finally, the new observation in the local range is integrated into the global map. The actual distance value is propagated outside the local range by parallel wavefront algorithms, and the global EDT can be obtained. After the construction of OGM and EDT, voxels in the map are labeled in three states, *occupied*, *free*, and *unknown*. Besides, each observed voxel records its distance from the closest obstacle. Hence, the motion planner will drive the vehicle towards the goal through the observed region while avoiding occupied grids.

We specially tailor the volumetric mapper for Air Bumper. The collision detection mechanism is modeled as a sensor that generates observations of an obstacle, which we refer to as a *collision sensor* in below. Upon receiving the point cloud from a collision sensor, the mapper uses a feature extractor from PCL to encapsulate all points to an OBB (oriented bounding box). The bounding vertices and corresponding transformation matrix associated with each collision-induced OBB are stored in the mapper and further streamed to GPU in OGM updating stage. After the local OGM is constructed with onboard sensor observation, the mapper inspects each voxel in parallel to check if the corresponding voxel should be set as occupied in the global OGM. In a thread dealing with the voxel v , all OBBs are iterated, and v is transformed into each OBB coordinate. If v is inside one of the OBBs marked by the collision sensor, or it is *occupied* in the local OGM, then the global OGM increases the occupancy probability of v . This indicates the collision sensor has a higher priority than onboard sensors, in that the obstacle registered by the collision sensor will not be cleared by onboard sensors. Local OGM is updated accordingly, and EDT takes the observation of the collision sensor as well. In consequence, the vehicle remembers all obstacles it ever collides with and will avoid them in future navigation.

D. Collision Reaction Motion Planning

Once the MAV platform detects the collision information, the motion planning will do re-planning based on the updated collision-aware OGM and EDT. Here we use the GTO-MPC [11] algorithm to plan a feasible trajectory to achieve the

pre-collision goal and avoid obstacles simultaneously. GTO-MPC algorithm is divided into two steps. Firstly, a jerk-limited trajectory is generated to supply the guiding time-optimal (GTO) initial solution. Then, an MPC-based method is applied to find the trajectory with considering obstacles, smoothness, and flight performance. In our framework, the optimization problem of the second step is formulated as the equation 10 to find the best trajectory $x(t), t \in [t_0, t_0 + T]$.

$$\begin{aligned}
 \min \quad & J = \int_{t_0}^{t_0+T} u^2(t) dt + w_1 \int_{t_0}^{t_0+T} \|x(t) - x_j(t)\|^2 dt \\
 & + w_2 \int_{t_0}^{t_0+T} e^{-\|d(t)\|} dt \\
 \text{s.t.} \quad & \dot{x}(t) = f(x(t), u) \\
 & x(t) \in \mathcal{X}_{\text{free}} \\
 & x^{(k)}(t) \in \Phi_k
 \end{aligned} \tag{10}$$

Where the first term of J minimizes the jerk (the derivative of acceleration) to encourage the smoothness of the trajectory, the second term is to minimize the errors between the state trajectory $x(t)$ and jerk limited trajectory. The third term penalizes the closest distance from the drone to obstacles in the EDT map. In the constraints, $f(\cdot)$ is the dynamic function of the quadrotor, $\mathcal{X}_{\text{free}}$ represents the free grids in the OGM, and Φ_k indicates the limited range of velocity, acceleration, and jerk. w_1 and w_2 are the weight coefficients for the corresponding term.

In general, the trajectory generation method achieves the re-planning frequency of 5Hz with a prediction horizon $T = 2s$ while guaranteeing kinodynamic feasibility, flight safety, and smoothness simultaneously. All of these great performances enable the MAV to react quickly to obstacles detected by the collision detection and estimation module.

VI. EXPERIMENTS AND RESULTS

A. Simulation in an Unknown Environment

We use a customized environment to evaluate the Air Bumper framework in the Gazebo [24] simulator, as shown in Fig. 5(a). In the customized environment, we use a simulated MAV with a Velodyne VLP-16 LiDAR sensor, which has 360° horizontal FOV, 30° vertical FOV, and the maximum sensing distance is 100m. Two kinds of doors are designed to validate the framework. One is a black door frame without any obstacles. The other one is a white door frame and transparent material, like glass, within the frame, and it is used to simulate a scenario with transparent obstacles. LiDAR is unable to detect transparent obstacles during flight. As a result, the motion planning module may generate a path from the current position to the next goal that passes through the white glass door. This could cause the MAV, without our framework, to become stuck or crash.

In the simulation test, we set three doors: two white doors with transparent obstacles located at $[0, -3, 1]^T$ m and $[0, -8, 1]^T$ m, and one black normal door at $[0, -13, 1]^T$ m. Once the start command is received, the drone takes off and flies autonomously through waypoints (WPs). It follows a path from the origin point $[0, 0, 1]^T$ m to the first waypoint (WP1) $[0, -5, 1]^T$ m, then to the second waypoint (WP2) $[0, -10, 1]^T$ m, and finally to the third waypoint (WP3)

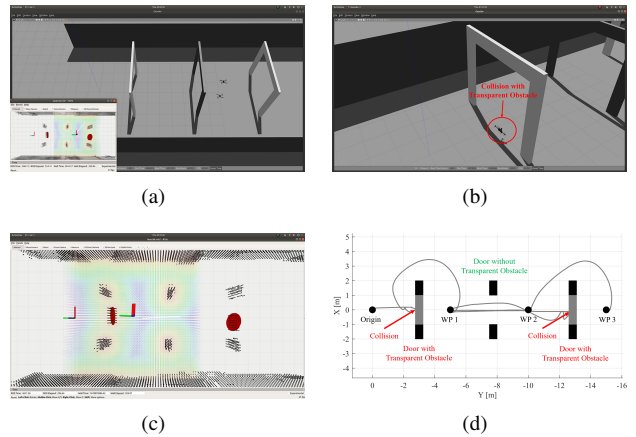


Fig. 5. MAV with Air Bumper successfully detects and recovers from collisions with two transparent obstacles in a simulation environment. (a) Overview of the customized environment. (b) MAV without our framework crashed due to the collision with a transparent obstacle. (c) Illustration of the collision-aware map. (d) The trajectory of the simulated MAV with Air Bumper framework.

$[0, -15, 1]^T$ m. Without our collision detection and reaction framework, the MAV collides with the transparent obstacles and crashes when passing through the white glass doors (Fig. 5(b)). In contrast, our Air Bumper framework enables the MAV rapidly recover from the collision upon detecting the abnormal acceleration data in the y direction. The collision-aware mapping module consequently updates the collision-aware map, where estimated obstacles are marked in red in Fig. 5(c). The collision-aware map assists the motion planning module in re-planning a smooth trajectory to the goal without colliding with the same obstacles (Fig. 5(d)). Results demonstrate that our framework is able to handle several collisions with unobserved obstacles during autonomous flight and record the collision information for further safe navigation.

B. Experiments in Real World

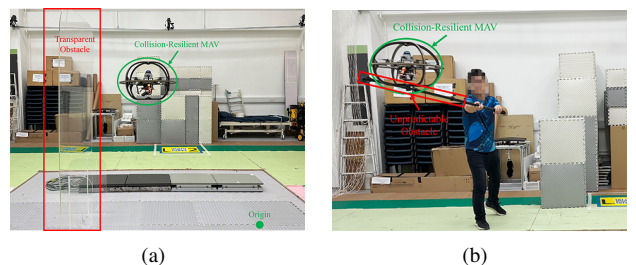


Fig. 6. The snapshots of testing Air Bumper in the unknown environment with (a) transparent and (b) unpredictable obstacles.

The Air Bumper framework's performance is demonstrated using the collision-resilient MAV designed in Section III-B in an unknown indoor environment with a transparent obstacle (Fig. 6(a)) and an unpredictable obstacle (Fig. 6(b)). The MAV is programmed to autonomously take off from the origin to the first waypoint (WP1) $[0.0, 0.0, 1.5]^T$ m, then fly towards the second waypoint (WP2) $[0.0, -3.5, 1.5]^T$ m,

and then perform back-and-forth flights between the two waypoints.

For the scenario with a transparent obstacle, a customized transparent object with a size of $2\text{ m} \times 1\text{ m}$ and a thickness of 8 mm is considered an obstacle. The bottom center of the obstacle is located at $[0.0, 1.7, 0.0]^T\text{ m}$. The OGM in Fig. 7(a), represented by the black point cloud, demonstrates that the laser beams are able to penetrate the transparent object. Therefore, there are no occupied voxels in the proximity of the obstacle's location, and the motion planning algorithm plans a path through the obstacle, which leads the MAV to collide with the transparent obstacle and easily get stuck or crash.

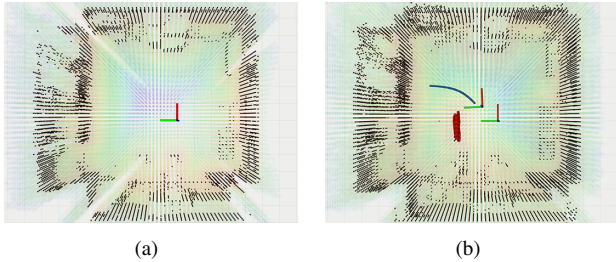


Fig. 7. The collision-aware map (a) before and (b) after a collision.

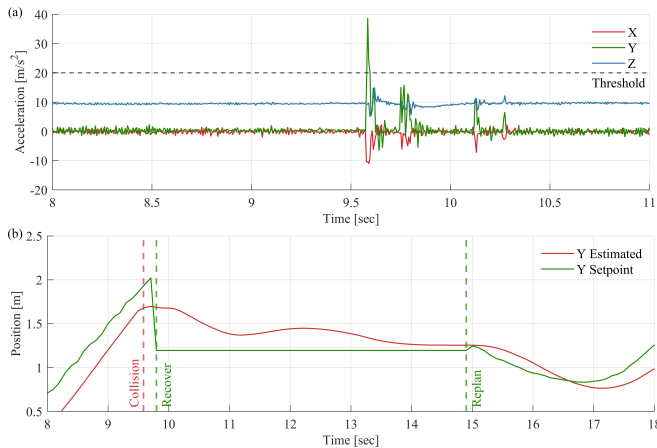


Fig. 8. States of the MAV before and after a collision with a transparent obstacle. (a) During the collision, acceleration on y -direction exceeds the detection threshold. (b) Position estimation and setpoints on y -direction.

In one of the flight tests, the collision generates an abnormal acceleration on the y -axis, exceeding the threshold, which occurred at approximately 9.58 seconds (Fig. 8). The collision is detected and estimated as bC with $\phi = 103.5^\circ$ and $\theta = 90.7^\circ$. Then the collision recovery control module calculates and generates a recovery position setpoint in the negative y -direction to move the drone away from the obstacle at around 9.79 seconds (Fig. 8). The recovery position ensures the drone is at a safe distance of approximately 0.5 meters from the obstacle. Meanwhile, the collision-aware map is updated after receiving the collision point cloud, marked red in Fig. 7(b). With the help of the collision-aware map, GTO-MPC re-plans a feasible trajectory to the second waypoint, which is shown as a blue line in Fig. 7(b), and

the low-level controller executes the re-planned setpoint at around 14.90 seconds (Fig. 8). The framework is designed to allow for a 5-second window after a collision has occurred for the motion planning algorithm to re-plan a feasible path. However, the actual time it takes for the drone to recover and stabilize after the collision is less than 1 second.

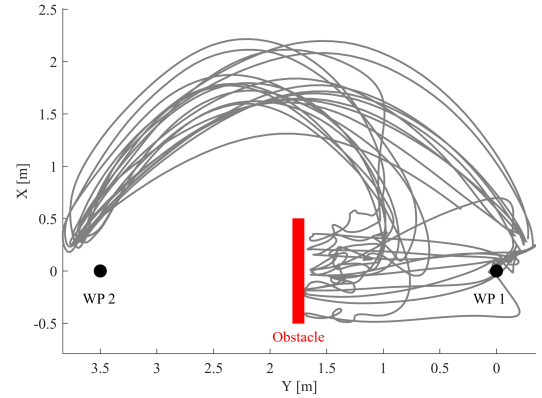


Fig. 9. Real experimental trajectories (ten trails) of the collision-resilient MAV with collision detection and reaction.

We then conduct ten trials to demonstrate the robustness of our framework for this case. All the experimental trajectories in the testing scenario are shown in Fig. 9. In all the trials, the collision-resilient drone collides with the transparent obstacle, and our framework successfully detects and reacts to the collision. Although some of the trajectories do not intersect with the obstacles, the maximum distance between the surface of the obstacle and the collision position is only 0.1 m, which still falls within the drone's radius.

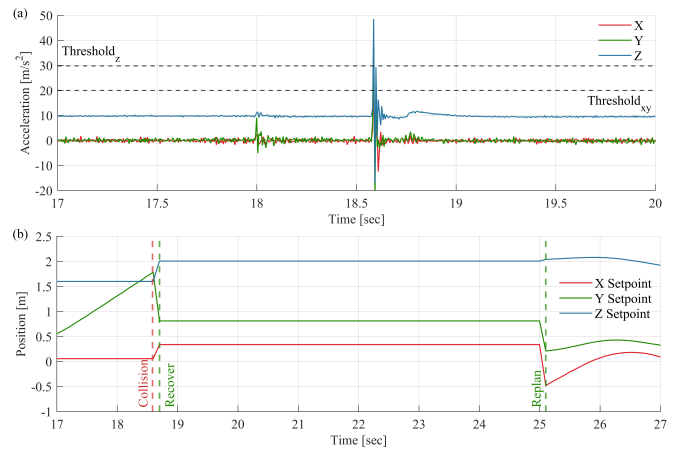


Fig. 10. States of the MAV before and after a collision with an unpredictable obstacle. (a) During the collision, accelerations exceed the collision detection threshold. (b) Position setpoints on three axes.

For the scenario with an unpredictable obstacle, we use a stick to randomly hit the MAV outside the FOV of the LiDAR to demonstrate the ability of the Air Bumper framework to detect the collision with unpredictable obstacles and perform reactions in 3D space. When the stick hits the MAV from the lower left side of the cage, there are abnormal acceleration data on all three axes (Fig. 10.a), and the collision is detected at 18.59 s. Then a 3D recovery

control is performed with setpoints on three axes at 18.70 s (Fig. 10.b), the recovery distance d ensures the drone is at a safe distance of approximately 0.5 m from the obstacle in the xy -plane and the recovery distance on z -axis, d_z , makes the drone ascend from 1.5 m to about 2 m. Results demonstrate that our framework enables the MAV to maintain a safe distance from the obstacle in 3D space rather than just in a certain plane. Then the collision-aware mapping module generates a collision point cloud at the collision point which helps the motion planning module generate a smooth feasible trajectory to the original waypoint successfully.

VII. CONCLUSION

In this work, we introduced a collision detection and reaction framework to help MAVs recover from collisions during autonomous flights in an unknown environment with unobserved obstacles. To do so, we designed an IMU-based collision detection and estimation module to estimate the collision intensity, direction, and position. Collision reaction modules are developed to assist the drone quickly away from the obstacle and update the collision-aware map to generate a smooth post-collision trajectory. In addition to the software, a caged collision-resilient MAV is also designed and fabricated which fully demonstrates the ability of our framework in the real world. The motion planning algorithm in the current framework still needs a certain time to re-plan after collisions. In the future, we aim to introduce collision-inclusive motion planning, which can better utilize collisions in autonomous navigation in complex environments. The framework can also be extended to assist multi-robot navigation in hazardous environments.

REFERENCES

- [1] T. Rakha and A. Gorodetsky, "Review of unmanned aerial system (uas) applications in the built environment: Towards automated building inspection procedures using drones," *Automation in Construction*, vol. 93, pp. 252–264, 2018.
- [2] B. Chan, H. Guan, J. Jo, and M. Blumenstein, "Towards uav-based bridge inspection systems: A review and an application perspective," *Structural Monitoring and Maintenance*, vol. 2, no. 3, pp. 283–300, 2015.
- [3] R. Montero, J. G. Victores, S. Martinez, A. Jardón, and C. Balaguer, "Past, present and future of robotic tunnel inspection," *Automation in Construction*, vol. 59, pp. 99–112, 2015.
- [4] M. Tranzatto, T. Miki, M. Dharmadhikari, L. Bernreiter, M. Kulkarni, F. Mascarich, O. Andersson, S. Khattak, M. Hutter, R. Siegwart, *et al.*, "Cerberus in the darpa subterranean challenge," *Science Robotics*, vol. 7, no. 66, p. eabp9742, 2022.
- [5] A. Agha, K. Otsu, B. Morrell, D. D. Fan, R. Thakker, A. Santamaria-Navarro, S.-K. Kim, A. Bouman, X. Lei, J. Edlund, *et al.*, "Nebula: Quest for robotic autonomy in challenging environments; team costar at the darpa subterranean challenge," *arXiv preprint arXiv:2103.11470*, 2021.
- [6] N. Hudson, F. Talbot, M. Cox, J. Williams, T. Hines, A. Pitt, B. Wood, D. Frousheger, K. L. Surdo, T. Molnar, *et al.*, "Heterogeneous ground and air platforms, homogeneous sensing: Team csiro data61's approach to the darpa subterranean challenge," *arXiv preprint arXiv:2104.09053*, 2021.
- [7] Y. Bi, M. Lan, J. Li, S. Lai, and B. M. Chen, "A lightweight autonomous mav for indoor search and rescue," *Asian Journal of Control*, vol. 21, no. 4, pp. 1732–1744, 2019.
- [8] J. Horyna, T. Baca, V. Walter, D. Albani, D. Hert, E. Ferrante, and M. Saska, "Decentralized swarms of unmanned aerial vehicles for search and rescue operations without explicit communication," *Autonomous Robots*, vol. 47, no. 1, pp. 77–93, 2023.
- [9] W. Xu, Y. Cai, D. He, J. Lin, and F. Zhang, "Fast-lid2: Fast direct lidar-inertial odometry," *IEEE Transactions on Robotics*, 2022.
- [10] C. Campos, R. Elvira, J. J. G. Rodríguez, J. M. Montiel, and J. D. Tardós, "Orb-slam3: An accurate open-source library for visual, visual-inertial, and multimap slam," *IEEE Transactions on Robotics*, vol. 37, no. 6, pp. 1874–1890, 2021.
- [11] L. Xi, X. Wang, L. Jiao, S. Lai, Z. Peng, and B. M. Chen, "Gto-mpc-based target chasing using a quadrotor in cluttered environments," *IEEE Transactions on Industrial Electronics*, vol. 69, no. 6, pp. 6026–6035, 2021.
- [12] S. Lai, M. Lan, and B. M. Chen, "Model predictive local motion planning with boundary state constrained primitives," *IEEE Robotics and Automation Letters*, vol. 4, no. 4, pp. 3577–3584, 2019.
- [13] C. J. Salaan, K. Tadakuma, Y. Okada, Y. Sakai, K. Ohno, and S. Tadokoro, "Development and experimental validation of aerial vehicle with passive rotating shell on each rotor," *IEEE Robotics and Automation Letters*, vol. 4, no. 3, pp. 2568–2575, 2019.
- [14] Z. Liu and K. Karydis, "Toward impact-resilient quadrotor design, collision characterization and recovery control to sustain flight after collisions," in *2021 IEEE International Conference on Robotics and Automation (ICRA)*. IEEE, 2021, pp. 183–189.
- [15] S. Wang, N. Anselmo, M. Garrett, R. Remias, M. Trivett, A. Christoffersen, and N. Bezzo, "Fly-crash-recover: A sensor-based reactive framework for online collision recovery of uavs," in *2020 Systems and Information Engineering Design Symposium (SIEDS)*. IEEE, 2020, pp. 1–6.
- [16] P. De Petris, H. Nguyen, M. Dharmadhikari, M. Kulkarni, N. Khedekar, F. Mascarich, and K. Alexis, "Rmf-owl: A collision-tolerant flying robot for autonomous subterranean exploration," in *2022 International Conference on Unmanned Aircraft Systems (ICUAS)*. IEEE, 2022, pp. 536–543.
- [17] C. Gao, X. Wang, R. Wang, Z. Zhao, Y. Zhai, X. Chen, and B. M. Chen, "A uav-based explore-then-exploit system for autonomous indoor facility inspection and scene reconstruction," *Automation in Construction*, vol. 148, p. 104753, 2023.
- [18] T. Lew, T. Emmei, D. D. Fan, T. Bartlett, A. Santamaria-Navarro, R. Thakker, and A.-a. Agha-mohammadi, "Contact inertial odometry: collisions are your friends," in *The International Symposium of Robotics Research*. Springer, 2019, pp. 938–958.
- [19] Y. Mulgaonkar, W. Liu, D. Thakur, K. Daniilidis, C. J. Taylor, and V. Kumar, "The tiercel: A novel autonomous micro aerial vehicle that can map the environment by flying into obstacles," in *2020 IEEE International Conference on Robotics and Automation (ICRA)*. IEEE, 2020, pp. 7448–7454.
- [20] Z. Lu, Z. Liu, M. Campbell, and K. Karydis, "Online search-based collision-inclusive motion planning and control for impact-resilient mobile robots," *IEEE Transactions on Robotics*, 2022.
- [21] G. Dicker, F. Chui, and I. Sharf, "Quadrotor collision characterization and recovery control," in *2017 IEEE International Conference on Robotics and Automation (ICRA)*. IEEE, 2017, pp. 5830–5836.
- [22] G. Dicker, I. Sharf, and P. Rustagi, "Recovery control for quadrotor uav colliding with a pole," in *2018 IEEE/RSJ International Conference on Intelligent Robots and Systems (IROS)*. IEEE, 2018, pp. 6247–6254.
- [23] Y. Chen, S. Lai, J. Cui, B. Wang, and B. M. Chen, "Gpu-accelerated incremental euclidean distance transform for online motion planning of mobile robots," *IEEE Robotics and Automation Letters*, 2022.
- [24] N. Koenig and A. Howard, "Design and use paradigms for gazebo, an open-source multi-robot simulator," in *2004 IEEE/RSJ International Conference on Intelligent Robots and Systems (IROS)*(IEEE Cat. No. 04CH37566), vol. 3. IEEE, 2004, pp. 2149–2154.